PAPER

Graphene foil as a current collector for NCM material-based cathodes

To cite this article: Huailiang Xu *et al* 2020 *Nanotechnology* **31** 205710

IOP Publishing Nanotechnology
Nanotechnology 31 (2020) 205710 (7pp) https://doi.org/10.1088/1361-6528/ab72ba

Graphene foil as a current collector for NCM material-based cathodes

Huailiang Xu[1], Hongchang Jin[1], Zhikai Qi[2], Yue Guo[1], Jinxi Wang[1], Yanwu Zhu[3] and Hengxing Ji[1]

[1] Hefei National Laboratory for Physical Sciences at the Microscale, Department of Applied Chemistry, CAS Key Laboratory of Materials for Energy Conversion, iChEM (Collaborative Innovation Center of Chemistry for Energy Materials), University of Science and Technology of China. Hefei 230026, People's Republic of China
[2] Key Laboratory of Magnetic Molecules and Magnetic Information Material of Ministry of Education, School of Chemistry and Material Science, Shanxi Normal University. Linfen 041004, People's Republic of China
[3] Department of Materials Science and Engineering, CAS Key Laboratory of Materials for Energy Conversion, iChEM (Collaborative Innovation Center of Chemistry for Energy Materials), University of Science and Technology of China. Hefei 230026, People's Republic of China

E-mail: jihengx@ustc.edu.cn

Received 9 November 2019, revised 18 January 2020
Accepted for publication 4 February 2020
Published 4 March 2020

Abstract

When used as a current collector, aluminum foil (AF) is vulnerable to local anodic corrosion during the charge/discharge process, which can lead to the deterioration of lithium-ion batteries (LIBs). Herein, a graphene foil (GF) with high electrical conductivity (~5800 S cm^{-1}) and low mass density (1.80 g cm^{-3}) was prepared by reduction of graphene oxide foil with ultra-high temperature (2800 °C) annealing, and it exhibited significantly anodic corrosion resistance when serving as a current collector. Moreover, a $LiNi_{0.5}Co_{0.2}Mn_{0.3}O_2$ (NCM523) cathode using GF as a current collector (NCM523/GF) demonstrated a gravimetric capacity of 137.3 mAh g^{-1} at 0.5 C based on the mass of the whole electrode consisting of the active material, carbon black, binder, and the current collector, which is 44.5% higher than that of the NCM523/AF electrode. Furthermore, the NCM523/GF electrode retains higher capacity at relatively faster rates, from 0.1 C to 5.0 C. Therefore, GF, a lightweight corrosion-resistant current collector, is expected to replace the current commercial metal current collectors in LIBs and to achieve high energy-density batteries.

Supplementary material for this article is available online

Keywords: graphene foil, current collector, lithium-ion batteries, capactiy

1. Introduction

The current collector is an essential part of lithium-ion batteries (LIBs). It supports the electrochemically active materials and transfers electrons between active materials and the external circuit [1]. An ideal current collector for LIBs should be electrochemically inactive, anticorrosive, highly conductive, lightweight and cost-effective. Typically, the extensively used materials for current collectors are Al foil (AF) for cathodes and Cu foil for anodes. However, both Al and Cu foils are susceptible to localized corrosion during long-term cycling because of the decomposition of lithium hexafluorophosphate ($LiPF_6$) and lithium bis (trifluoromethane sulfonyl) imide (LiTFSI) [2–8], which leads to a loss of specific capacity. Therefore, finding one material which can satisfy both the physics requirements and high utility in an LIB system is highly significant.

To this end, a great deal of effort has been made to optimize current collectors. Carbon materials have been researched as current collectors because of their low density and high conductivity. Especially, carbon materials are resistive to chemical corrosion within a wide range of electrochemical window. Graphene-coating methods have been reported, which effectively prevents the corrosion of metal

current collectors and improves battery performance [9–11]. Three-dimensional (3D) carbon current collectors can form an interconnected electron conductive path to significantly improve the rate capability while maintaining excellent electrochemical stability [12–15]. Two-dimensional (2D) carbon films, such as graphite foil [16], carbon nanotube (CNT) film [17–20] and graphene film [21–27] have been reported to replace the metal current collectors in LIBs. These results indicate the great potential of carbon-based materials for current collectors in LIBs. However, it is still rare to find a carbon-based current collector that is competitive with metal foils in terms of electrical conductivity, mechanical strength and production scalability.

In this work, we developed a blade-coating method followed by high temperature (2800 °C) graphitization to efficiently produce a large graphene foil (GF) from graphene oxide. The GF has a thickness of micrometers, a length of meters and a width of tens of centimeters with high electrical conductivity (~5800 S cm^{-1}), low mass density (1.80 g cm^{-3}), excellent tensile strength (90 MPa) and anodic corrosion resistance. These physical properties yield the GF to be a competitive material for use as the current collector in LIBs. The cathode materials, $LiNi_{0.5}Co_{0.2}Mn_{0.3}O_2$ (NCM523), $LiNi_{0.6}Co_{0.2}Mn_{0.2}O_4$ (NCM622) and $LiFePO_4$ (LFP) loaded on the GF demonstrated an enhanced gravimetric capacity when calculated based on the mass of the whole electrode including the active material, binder and conductive additives, and current collector, together with improved cycling stability and rate capability.

2. Experimental

2.1. Preparation of the GF

The graphene oxide was prepared through the modified Hummer's method, which was dispersed in water to form a graphene oxide colloidal suspension (25 mg ml^{-1}). The suspension was then coated on a polyethylene terephthalate (PET) substrate through blade coating, and dried at 100 °C, which was followed by thermal annealing at 2800 °C in argon flow. A GF of meters in length and tens of centimeters in width could be obtained.

2.2. Electrochemical measurements

The GF and AF with areal masses of 2.0 and 6.4 mg and thicknesses of 12 and 22 μm, respectively, were directly used as current collectors without any pretreatment. $LiNi_{0.5}Co_{0.2}Mn_{0.3}O_2$ (NCM523, Beijing Easpring Material Technology Co., Ltd), $LiNi_{0.6}Co_{0.2}Mn_{0.2}O_4$ (NCM622, Beijing Easpring Material Technology Co., Ltd) or $LiFePO_4$ (LFP; Tianjin BTR New Energy Materials Co., Ltd) powder (9.0 g) was mixed with polyvinylidene fluoride (PVDF; Shanghai 3F New Materials Technology Co., Ltd, 0.5 g) and super P carbon (Jiaozuo City Hexing Chemical Industry Co., Ltd, 0.5 g) in 1-methyl-2-pyrrolidone (NMP) to formulate a slurry, which was then blade coated on GF or AF current collectors. The electrodes were sequentially dried in a drum wind oven at 80 °C for 4 h before drying in a vacuum oven at 110 °C for 8 h. Finally, the electrodes were cut into disks of diameter of 1.2 cm, which were coupled with lithium metal foils as an anode to assemble 2032 type coin cells. An 80 μl electrolyte, containing 1 M $LiPF_6$ dissolved in ethylene carbonate, ethyl methyl carbonate and dimethyl carbonate (EC: EMC:DMC = 1:1:1 in volume, Zhangjiagang Guotai Huarong Chemical New Material Co., Ltd), was added to each cell. The mass loading of the active material was around 8.0 mg cm^{-2} on the current collector. The density of the electrode was around 2.1 g cm^{-3} on the current collector. The cells were aged for 8 h before electrochemical tests. The gravimetric capacity values reported in this work are calculated with respect to the mass of the whole electrode containing active material, additives and current collector.

Herein, we mainly studied the effect of using GF as a current collector on battery performance. In addition, due to the light weight of the GF, the loading of cathode materials is also different from the practical application. Therefore, there is no in-depth study on the loading of cathode material in this work.

The cyclic voltammetry (CV) and electrochemical impedance spectral (EIS) measurements were carried out on a Princeton electrochemical workstation (PARSTAT4000A). CV was performed at a scan rate of 10 mV s^{-1} in the potential range of 2.0–5.0 V (versus Li/Li^+). The EIS studies were performed before and after cycling of the electrodes in the frequency range of 500 kHz–0.01 Hz at open circuit potential conditions. Galvanostatic charge–discharge experiments were performed at different current densities in the potential range of 2.8–4.5 V (versus Li/Li^+) using a CT2001A cell test instrument (Land Electronic Co., Ltd).

The energy density of the electrodes was calculated according to the following equation: energy density = (specific capacity × discharge voltage platform)/M_w, where M_w is the sum of the mass of active material, additives and current collector, and the negative electrode is lithium.

2.3. Characterization

The scanning electrical microscopy (SEM) images of the GF were obtained with JSM-2100F (JEOL Ltd) apparatus operated at 10.0 kV. The Raman spectra of the GF on SiO_2/Si substrate were measured by using Renishaw inVia equipment with a 532 nm laser and a ×50 objective lens. X-ray diffraction (XRD; D/max-TTR III) was performed with Cu Kα radiation (V = 40 kV, I = 200 mA). The tensile strength of the GF was obtained by using a peel strength tester (Dongguan PERFECT Instrument Co., LTD, PT-6081B). The tensile specimens have a gauge length of 10 cm, thickness of 12 μm and width of 1.0 cm. The flexibility of the GF was measured by Mit Folding Endurance Tester (GOTECH Testing Machines Inc., GT-6014-A MIT). The electrical conductivity of the GF (length of 4.9 cm, width of 1.9 cm and thickness of ~12 μm) was measured by using a four-probe method using a Keithley SCS 4200 semiconductor characterization system.

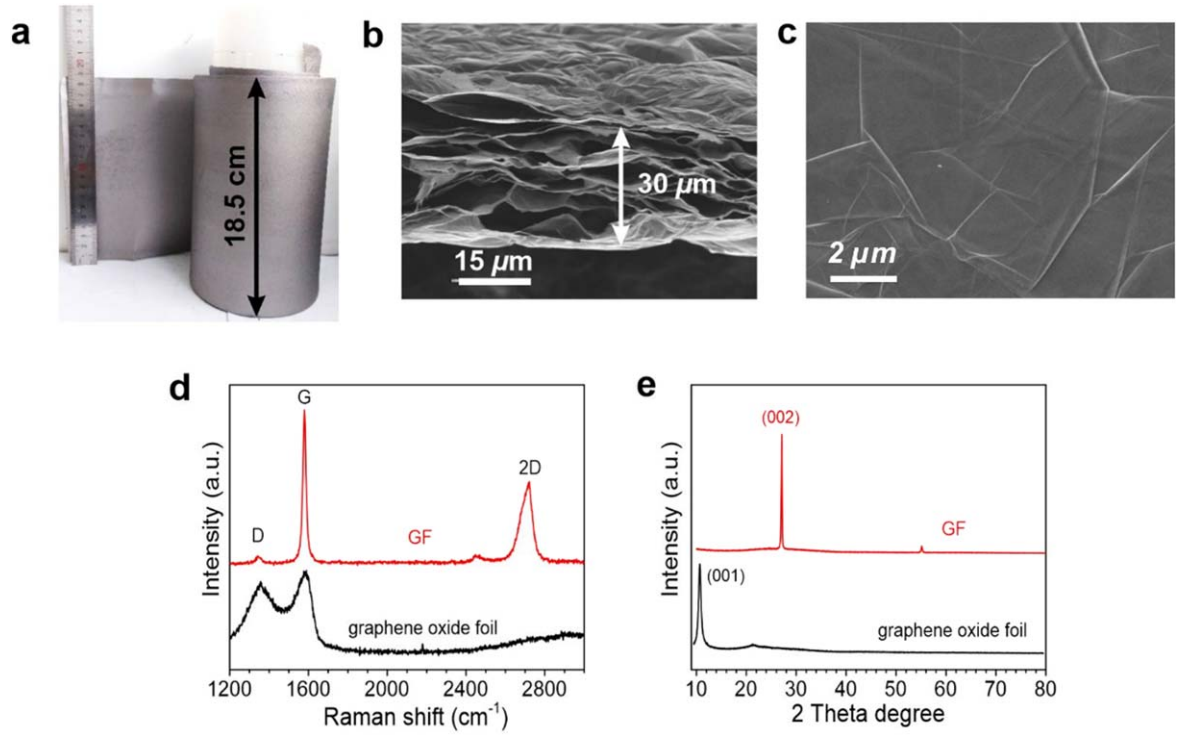

Figure 1. (a) Photograph of the GF; (b) before compression, the cross-sectional and (c) surface SEM images of the GF; (d) Raman spectroscopy of the graphene oxide foil and the GF, the low D/G ratio and the high 2D peak indicate highly crystalline GF after the graphitization process. (e) XRD patterns of the graphene oxide foil and the GF.

3. Results and discussion

Figure 1(a) presents the macroscale image of a GF with length of 20 meters and width of 18.5 cm. The SEM image in figure 1(b) shows that the GF contains a layer-by-layer stacking of graphene sheets with thickness of ~30 μm. Figure 1(c) shows the intrinsic wrinkles on the GF surface. After statistic compression under a pressure of 60 MPa, the density of the GF is about 1.80 g cm^{-3}. Moreover, we studied the compositional and structural evolutions from graphene oxide foil to GF by Raman spectroscopy and XRD. The Raman spectroscopy images in figure 1(d) show that both the graphene oxide foil and the GF have a D peak at 1365 cm^{-1} and a G peak at 1580 cm^{-1}. In addition, the GF has a 2D peak at 2716 cm^{-1}, and a lower intensity ratio of D peak to G peak (I_D/I_G) of ~0.09. This result proved that the GF obtained by high temperature annealing was of high quality [27–29]. Moreover, the XRD pattern of the graphene oxide foil shows a typical sharp and strong (001) peak at 2θ of 10.6°, corresponding to an interplanar spacing of 0.834 nm (figure 1(e)). Further analysis of the XRD pattern shows that the GF features a narrow and sharp intensity peak at around 26.6° corresponding to the (002) plane, and the interplanar spacing of the GF is about 0.335 nm, which is consistent with that of natural graphite [30]. The decrease in the interplanar spacing is due to the elimination of interlamellar water and some oxygen-containing groups. These results demonstrate that the ordered lamellar structure of the GF is well-preserved after the graphitization treatment.

The electrical conductivity of the GF obtained in this work is about 5800 S cm^{-1} (figure 2(a), see the Experimental section for details). Therefore, the conductivity of the as-prepared GF is much higher than that of the reported carbon films, such as graphene film prepared by chemical vapor deposition (CVD) method [27], reduced graphene oxide film [21, 26, 31], CNT film [18, 19], graphite foam [12] and graphite foil [16]. Moreover, we carried out tensile experiment by using a peel strength tester to further evaluate the capacity of the GF to withstand tensile loads. The stain–stress curve of GF recorded in figure 2(b) reveals an average tensile strength of 90 MPa at the breakage elongation of 2.6%. The Young's modulus of the GF with 10 cm gauge length and 1 cm gauge width was measured as 162.8 MPa.

$LiPF_6$ salt in Li-ion battery electrolytes decomposed with the presence of H_2O, generating HF [32]. To accelerate the corrosion of the current collector, we added 10 ppm of DI water into the electrolyte (1 M $LiPF_6$) and measured the cyclic voltammetry (CV) at 10 mV s^{-1}. Since we added 10 ppm of water into electrolyte, we chose 5.0 V to verify the electrochemical stability of the GF as the current collector. As shown in figure 3(a), the CV scan results showed obvious redox peaks for the AF in around 2.3 V (versus Li/Li^+), 3.3 V (versus Li/Li^+) and 3.3 V (versus Li/Li^+) at the first, the fifth and the tenth cycle, respectively, and no obvious redox peaks were observed for the GF (figure 3(c)). Then, we carefully took the current collectors out of the cells and checked their morphology after CV measurements. The SEM image clearly show that big cavities were formed by corrosion on the surface of the AF after ten CV cycles (figures 3(b) and

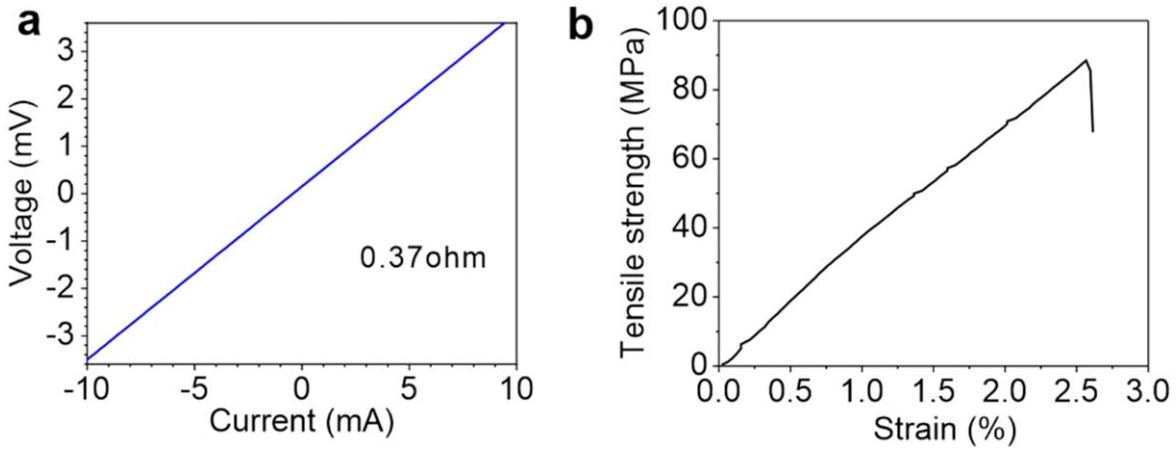

Figure 2. Electrical conductivity of (a) the GF and (b) tensile strength of the GF as a function of strain.

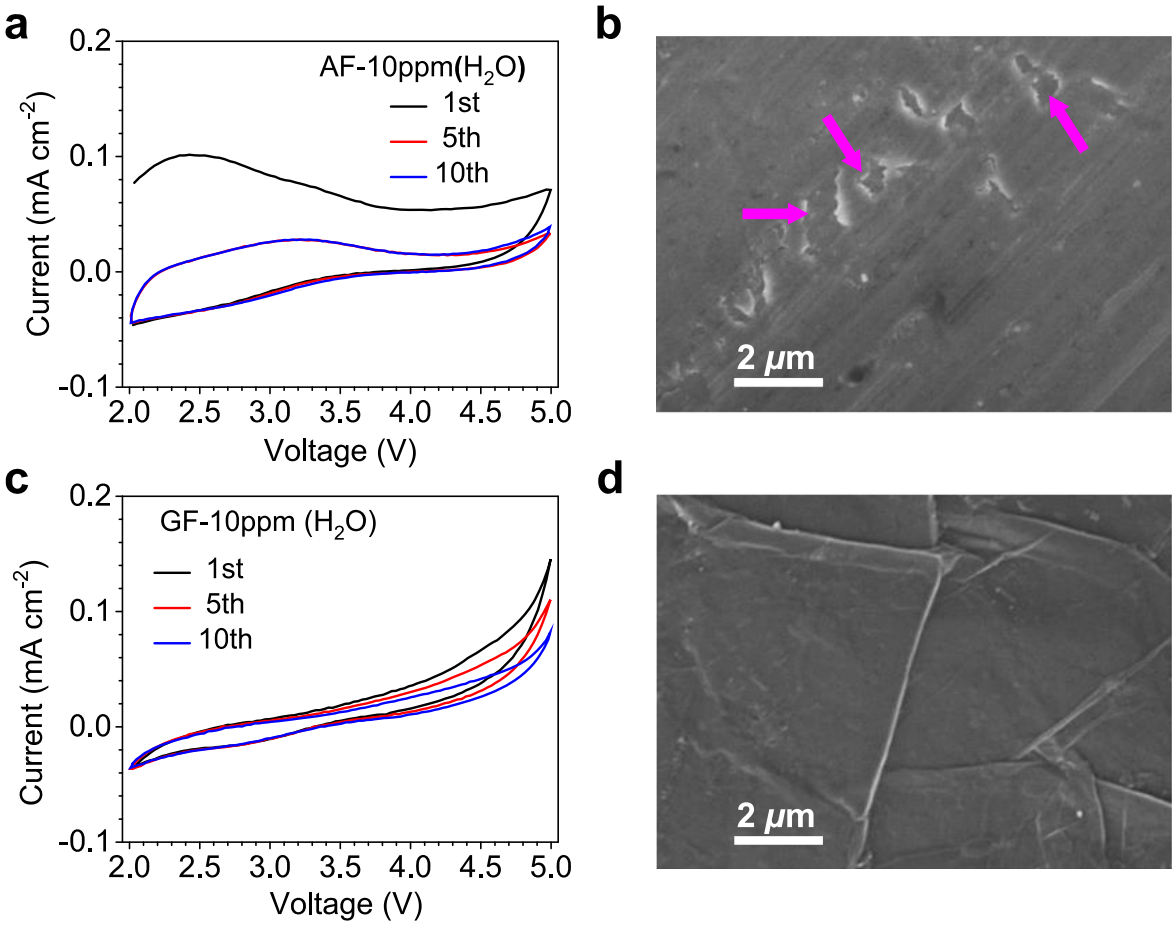

Figure 3. CV of the (a) AF and (c) the GF, SEM image of the (b) AF and (d) the GF after ten CV cycles.

S1 is available online at stacks.iop.org/NANO/31/205710/mmedia), while the GF had no obvious changes (figures 3(d) and 1(c)). Based on the above observations, we therefore conclude that the GF current collector has better electrochemical stability compared with the commercial AF current collector.

We further employ the obtained GF as cathode current collector for electrochemical experiments. As shown in figure 4(a), the as-prepared NCM523/GF electrode shows a good flexibility. Figure 4(b) shows that the active materials closely adhere to the surface of the GF. The electrochemical impedance spectroscopy (EIS) results, as show in figures 4(c)–(d) and table S1, reveal that before cycling (see experimental section for details) the NCM523/GF electrode has a lower charge transfer resistance (R_{ct}, 250 Ω) than that of NCM523/AF (950 Ω). These results indicate that the GF reduces the barrier of charge transfer between the electrode material and the current collector, which may enhance the

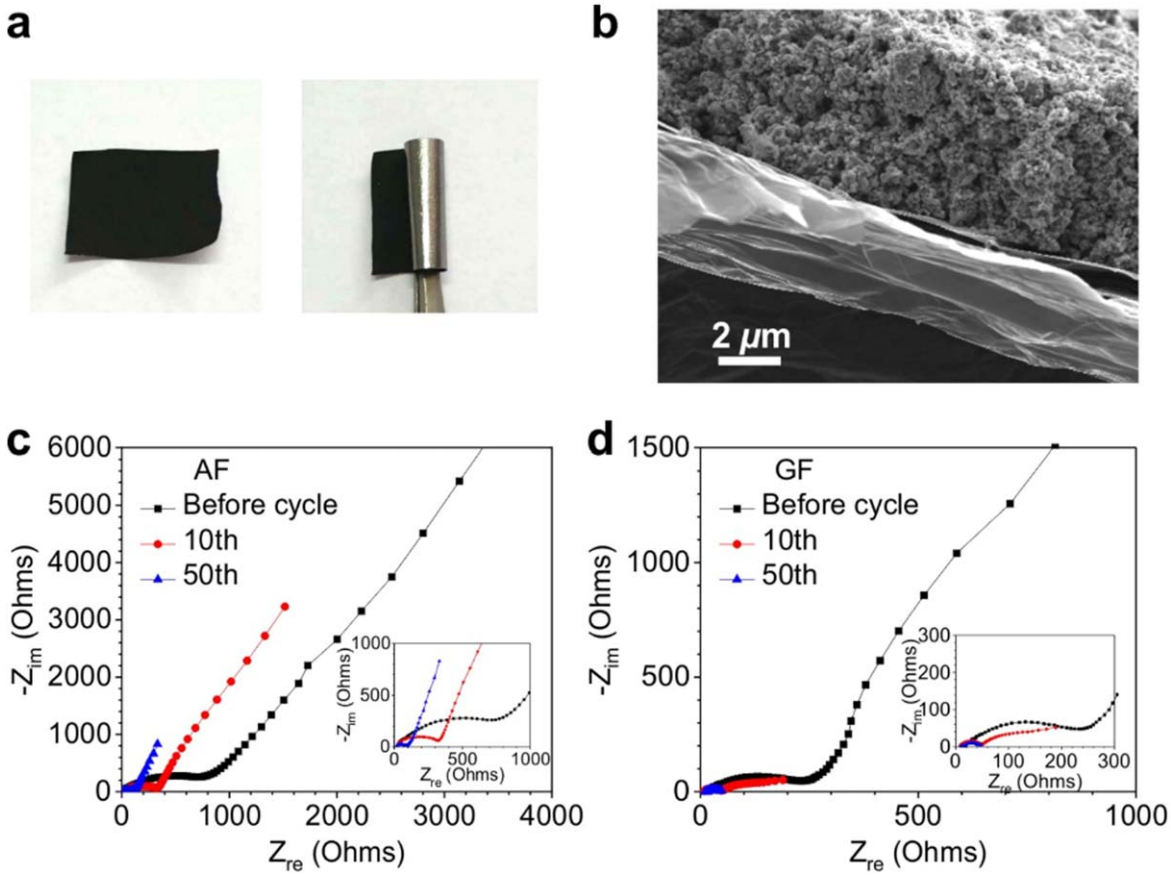

Figure 4. (a) Photography of the NCM523/GF electrode, (b) SEM image of the NCM523/GF electrode, (c) and (d) EIS analysis of cells.

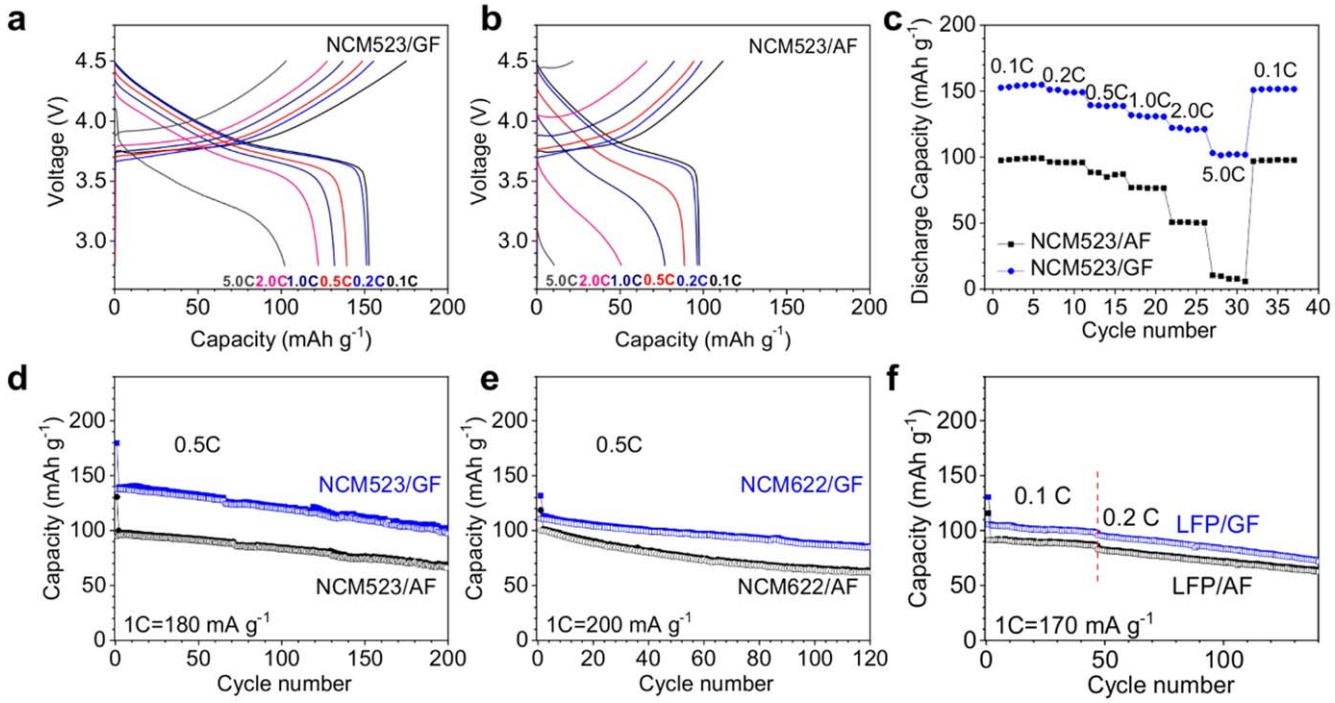

Figure 5. (a)–(b) Corresponding charge/discharge curves of cells, (a) NCM523/GF, (b) NCM523/AF; (c) rate performances of cells; and (d)–(f) long-term low-rate cycling performance of cells, (d) NCM523 (1C = 180 mA g^{-1}), (e) NCM622 (1C = 200 mA g^{-1}), (f) LFP (1C = 170 mA g^{-1}), respectively.

Table 1. The energy densities of NCM523/AF and NCM523/GF at different C rates.

Energy density						
	Energy density of NCM523 (Wh kg^{-1})					
Current collector	0.1C	0.2C	0.5C	1.0C	2.0C	5.0C
GF	635.4	626.9	569.9	536.0	486.8	383.3
AF	419.0	406.2	357.5	295.6	178.5	33.2

utilization of cathode materials at high rates [11, 33]. Furthermore, after 50 cycles, the R_{ct} of NCM523/GF (28 Ω) is still lower than that of NCM523/AF (70 Ω), which indicates the good interface between MCN532 and GF after long cycles, improving the overall performance of the electrode.

The galvanostatic charge and discharge experiments show that the polarization of NCM523/GF is much smaller than that of NCM523/AF in the high current density regime (figures 5(a), (b)). Further results in figure 5(c) reveal that the GF current collector has a better rate capacity than the AF current collector. Figures 5(d) and S2 show the cycling performance of the NCM523/GF and NCM523/AF electrodes. The initial discharge-specific capacities of the NCM523/GF were 137.3, 123.3 and 112.4 mAh g^{-1} at 0.5, 2.0 and 5.0 C (based on the mass of the whole electrode), respectively. After cycling for 200 cycles, the specific capacities of NCM523/GF decayed to 98.0, 59.3 and 42.0 mAh g^{-1} at 0.5 C, 2.0 C and 5.0 C, respectively, but they are much higher than that of NCM523/AF (66.2, 50.5 and 10.6 mAh g^{-1}). The cycling data are re-plotted by replacing 22 μm AF with 15 μm AF using current electrochemical data, as shown in figure S3. The results demonstrate that the electrochemical performance of the cell with 15 μm AF as a current collector is slightly better than that with 22 μm AF. If we only count the mass of the active material, the initial specific capacities of the NCM523/GF electrode and the NCM523/AF electrode are 170.2 mAh g^{-1} and 154.7 mAh g^{-1}, respectively (figures S4 and S5). Similarly, the cells with the GF current collector have better electrochemical performance, including rate performance and long-term cycling performance. Additionally, we also calculated the energy density of NCM523/AF and NCM523/GF, as shown in table 1. The NCM523/GF current collector shows a higher energy density of 635.4 Wh kg^{-1} at 0.1 C than NCM523/AF (419.0 Wh kg^{-1} at 0.1 C), especially at the high rate of 5.0 C; NCM523/GF delivers an energy density of 383.3 Wh kg^{-1}. Accordingly, the GF current collector is able to enhance the rate/power performance of LIBs.

Aside from its obvious role as a current collector for NCM523 materials, the capacities of NCM622 materials (figure 5(e)) and LFP (figure 5(f)) materials with the GF current collector were also improved compared with te AF current collector. Since the GF current collector weighs less than conventional metal current collectors, the weight of LIBs could be efficiently reduced. The energy density of these electrodes was also calculated, as shown in table 2. The GF current collector also shows higher energy density than that of the AF current collector. To sum up, we demonstrate a design of high energy-density battery, which shows potential to be scaled up for industrial applications.

Table 2. The energy densities of AF and GF current collectors with different cathode materials.

Cycle number					
		Energy density (Wh kg^{-1})			
Samples		1st	100th	120th	200th
NCM523 (0.5 C)	GF	531.9	448.2	429.7	349.8
8.0 mg cm^{-2}	AF	362.1	304.5	294.2	236.8
NCM622 (0.5 C)	GF	928.6	740.4	715.9	/
4.0 mg cm^{-2}	AF	568.2	340.7	324.4	/
LFP (0.1 C)	GF	522.3	399.1	374.2	/
7.2 mg cm^{-2}	AF	436.9	324.3	305.6	/

4. Conclusion

In conclusion, the GF current collector exhibited excellent electrochemical stability and significantly improved cyclic stability and electrode energy density compared to the AF current collector. The electrochemical stability of the GF current collector for LIBs has been proved and found to provide lightweight corrosion resistance. More importantly, our studies clearly show that GF current collector has better electrochemical performance, including rate performance, long-term cycling performance and energy-density under a high current density. The GF current collector offers a new option for high-performance and high energy-density LIBs.

Acknowledgments

This work was supported by the Natural Science Foundation of China (51761145046), and the 100 Talents Program of the Chinese Academy of Sciences.

Conflict of interest

All authors declare that there are no conflicts of interest.

ORCID iDs

Hengxing Ji https://orcid.org/0000-0003-2851-9878

References

[1] Goodenough J B 2012 Evolution of strategies for modern rechargeable batteries *Acc. Chem. Res.* **46** 1053–61

[2] Larry J, Krause W L, John S, Mark E, Gary K, Robert L and Radoslav A 1997 Corrosion of aluminum at high voltages in non-aqueous electrolytes containing perfluoroalkylsulfonyl imides; new lithium salts for lithium-ion cells *J. Power Sources* **68** 320–5

[3] Jeffrey W, Braithwaite A G, Ganesan N, Samuel J L, Diane E P, James A O and Wendy R C 1999 Corrosion of lithium-ion battery current collectors *J. Electrochem. Soc.* **146** 448–56

[4] Zhang S S and Jow T R 2002 Aluminum corrosion in electrolyte of Li-ion battery *J. Power Sources* **109** 458–64

[5] Zhang X, Winget B, Doeff M, Evans J W and Devine T M 2005 Corrosion of aluminum current collectors in lithium-ion batteries with electrolytes containing $LiPF_6$ *J. Electrochem. Soc.* **152** B448–54

[6] Shu J, Shui M, Huang F T, Xu D, Ren Y L, Hou L, Cui J and Xu J J 2011 Comparative study on surface behaviors of copper current collector in electrolyte for lithium-ion batteries *Electrochim. Acta* **56** 3006–14

[7] Kim Y S *et al* 2014 Succinonitrile as a corrosion inhibitor of copper current collectors for overdischarge protection of lithium ion batteries *ACS Appl. Mater. Interfaces* **6** 2039–43

[8] Myung S T, Hitoshi Y and Sun Y K 2011 Electrochemical behavior and passivation of current collectors in lithium-ion batteries *J. Mater. Chem.* **21** 9891–912

[9] Jiang J, Nie P, Ding B, Wu W, Chang Z, Wu Y, Dou H and Zhang X 2016 Effect of graphene modified Cu current collector on the performance of $Li_4Ti_5O_{12}$ anode for lithium-ion batteries *ACS Applied Materials & Interfaces* **8** 30926–32

[10] Kim H R and Choi W M 2018 Graphene modified copper current collector for enhanced electrochemical performance of Li-ion battery *Scr. Mater.* **146** 100–4

[11] Wang M *et al* 2017 Graphene-armored aluminum foil with enhanced anticorrosion performance as current collectors for lithium-ion battery *Adv. Mater.* **29** 1703882

[12] Ji H X, Zhang M T, Li H, Chen S, Shi L, Piner R and Ruoff R S 2012 Ultrathin graphite foam: a three-dimensional conductive network for battery electrodes *Nano Lett.* **12** 2446–51

[13] Li N, Chen Z, Ren W, Li F and Cheng H M 2012 Flexible graphene-based lithium ion batteries with ultrafast charge and discharge rates *PNAS* **109** 17360–5

[14] Hsu C H, Lin H H, Liu Y H and Lin H P 2018 Carbon fibers as three-dimensional current collectors for silicon/reduced graphene oxide lithium ion battery anodes with improved rate performance and cycle life *New J. Chem.* **42** 9058–64

[15] Pender J P, Xiao H, Dong Z, Cavallaro K A, Weeks J A, Heller A, Ellison C J and Mullins C B 2018 Compact lithium-ion battery electrodes with light weight reduced graphene oxide/Poly(Acrylic Acid) current collectors *ACS Appl. Energy Mater.* **2** 905–12

[16] Yazici M, Krassowski D and Prakash J 2005 Flexible graphite as battery anode and current collector *J. Power Sources* **141** 171–6

[17] Hu L B, Wu H, Mantia F L, Yang Y and Cui Y 2010 Thin, flexible secondary li-ion paper *Batteries. ACS Nano* **4** 5843–8

[18] Sun Z, Jin S, Jin H, Du Z, Zhu Y, Cao A, Ji H and Wan L J 2018 Robust expandable carbon nanotube scaffold for ultrahigh-capacity lithium-metal anodes *Adv. Mater.* **30** e1800884

[19] Yao Y *et al* 2018 Epitaxial welding of carbon nanotube networks for aqueous battery current collectors *ACS Nano* **12** 5266–73

[20] Neta Y, Mahmud A, Nina S and Yair E E 2018 Carbon nanotube tissue as anode current collector for flexible Li-ion batteries—understanding the controlling parameters influencing the electrochemical performance *APL Mater.* **6** 111102

[21] Gwon H, Kim H S, Lee K U, Seo D H, Park Y C, Lee Y S, Ahn B T and Kang K 2011 Flexible energy storage devices based on graphene paper *Energy & Environmental Science* **4** 1277–83

[22] Hu Y H, Li X F, Wang J J, Li R Y and Sun X L 2013 Free-standing graphene–carbon nanotube hybrid papers used as current collector and binder free anodes for lithium ion batteries *J. Power Sources* **237** 41–6

[23] Jiao L, Sun Z, Li H Y, Li F H, Wu T S and Niu L 2017 Collector and binder-free high quality graphene film as a high performance anode for lithium-ion batteries *RSC Adv.* **7** 1818–21

[24] Lee J K, Smith K B, Hayner C M and Kung H H 2010 Silicon nanoparticles-graphene paper composites for Li ion battery anodes *Chem. Commun.* **46** 2025–7

[25] Ning G, Xu C, Cao Y, Zhu X, Jiang Z, Fan Z, Qian W, Wei F and Gao J 2013 Chemical vapor deposition derived flexible graphene paper and its application as high performance anodes for lithium rechargeable batteries *J. Mater. Chem.* A **1** 408–14

[26] Chen Y *et al* 2016 Reduced graphene oxide films with ultrahigh conductivity as Li-ion battery current collectors *Nano Lett.* **16** 3616–23

[27] Cui L F, Wang X P, Chen N, Zhang G F and Qu L T 2017 A versatile graphene foil *J. Mater. Chem.* A **5** 14508–13

[28] Ferrari A C and Basko D M 2013 Raman spectroscopy as a versatile tool for studying the properties of graphene *Nat. Nanotechnol.* **8** 235–46

[29] Dresselhaus M S, Jorio A, Hofmann M, Dresselhaus G and Saito R 2010 Perspectives on carbon nanotubes and graphene Raman spectroscopy *Nano Lett.* **10** 751–8

[30] Li Z Q, Lu C J, Xia Z P, Zhou Y and Luo Z 2007 X-ray diffraction patterns of graphite and turbostratic carbon *Carbon* **45** 1686–95

[31] Zhang M, Wang Y, Huang L, Xu Z, Li C and Shi G 2015 Multifunctional pristine chemically modified graphene films as strong as stainless steel *Adv. Mater.* **27** 6708–13

[32] Lux S F, Lucas I T, Pollak E, Passerini S, Winter M and Kostecki R 2012 The mechanism of HF formation in $LiPF_6$ based organic carbonate electrolytes *Electrochem. Commun.* **14** 47–50

[33] Su Y S and Manthiram A 2012 Lithium–sulphur batteries with a microporous carbon paper as a bifunctional interlayer *Nat. Commun.* **3** 1166